ORIGINAL ARTICLE

Generation of Human Schwann Cells Through Non-Integrating Lentiviral (NILV) Reprogramming of Human Fibroblasts for Peripheral Nerve Regeneration

Muhamad Razin Mohd Razali[1], Ahmad Najib Hasan[1], Aisya Falaini Roslan[2], Nur Jannaim Muhamad[2], Julaina Abdul Jalil[2], Muhammad Fauzi Daud[1]*, Izyan Mohd Idris[2]

[1] Institute of Medical Science Technology, Universiti Kuala Lumpur (UniKL), A1-1, Jalan TKS 1, Taman Kajang Sentral, Selangor, 43000 Kajang, Selangor, Malaysia.
[2] Institute for Medical Research (IMR), National Institutes of Health (NIH), Ministry of Health Malaysia, Jalan Setia Murni U13/52, Seksyen U13 Setia Alam, 40170 Shah Alam, Selangor Darul Ehsan, Malaysia.

ABSTRACT

Introduction: Schwann cells are essential for peripheral nerve function and regeneration, but their limited availability presents a significant challenge for research and therapeutic applications. Direct reprogramming of fibroblasts into Schwann cells offers a promising alternative. This study aims to develop a reliable method for Schwann cell generation using non-integrating lentiviral vectors (NILVs) to enhance safety and efficiency. **Materials and Methods:** Lentiviral plasmids carrying SOX10 and EGR2 were cloned and validated by Sanger sequencing. NILVs encoding SOX10, EGR2, and eGFP were produced and assessed for transduction efficiency. BJ fibroblasts were transduced with NILV-SOX10 and NILV-EGR2, and their morphological changes were monitored over 21 days. Immunocytochemistry was performed on days 14 and 21 post-transduction to evaluate Schwann cell marker expression. **Results:** NILV successfully transduced BJ fibroblasts, leading to the expression of SOX10 and EGR2. Immunocytochemistry revealed S100β expression at 14 days post-transduction, suggesting an initial Schwann cell-like phenotype. However, SOX10 and MBP expression remained low, and by day 21, a decline in S100β expression was observed, indicating challenges in maintaining Schwann cell identity. **Conclusion:** NILV-based reprogramming effectively initiated Schwann cell-like transformation but was insufficient for stable lineage commitment. The gradual loss of Schwann cell markers suggests a need for further optimization, such as enhancing transgene stability or refining culture conditions, to improve long-term Schwann cell maintenance for peripheral nerve regeneration studies.
Malaysian Journal of Medicine and Health Sciences (2026) 22(SUPP3): 118-126. doi:10.47836/mjmhs.22.s3.18

Keywords: Direct cell reprogramming, transcription factor, SOX10, EGR2, schwann cells

Corresponding Author:
Muhammad Fauzi Daud, PhD
Email: mfauzid@unikl.edu.my
Tel: +603-8739 5894

INTRODUCTION

Schwann cells, the most abundant glial cells in the peripheral nervous system, play a crucial role in axonal support by forming myelin sheaths in myelinated fibers or Remak bundles in unmyelinated ones functions (1). Beyond structural support, they contribute to neurotrophic signaling (2), sensory modulation, synaptic function (3,4), and immune responses (5). Their remarkable plasticity is particularly significant in nerve injury repair and demyelinating diseases (6–8). As a result, Schwann cells hold great potential for regenerative cell transplantation and as an experimental model for understanding peripheral nerve biology and therapeutic development (9,10).

However, studying human Schwann cells (hSCs) remains challenging due to limited access and difficulties in obtaining human samples. As a result, rodent Schwann cells are widely used for in vitro studies due to their ease of culture, scalability, and sustained proliferation (11). Despite their utility in research, their applicability to human biology is under scrutiny, and ethical concerns persist regarding animal-derived cells (12).

Traditional human Schwann cell cultures face challenges such as limited availability, high variability, and ethical constraints (13). These cultures require labor-intensive techniques and exhibit restricted proliferation due to replicative senescence, making them less viable for clinical applications (14). Advances in stem cell

technology have allowed the derivation of hSCs from human induced pluripotent stem cells (iPSCs) (15), but this approach remains hindered by long differentiation times, genomic instability, and limited reprogramming efficiency (16).

An alternative strategy, direct cell reprogramming (transdifferentiation), has gained traction for generating hSCs efficiently. Studies have demonstrated that transcription factors such as SOX10 and EGR2 can reprogram human dermal fibroblasts into Schwann cells with conversion efficiencies of 12–40% (17,18). However, conventional lentiviral vectors pose risks of genomic integration and mutagenesis.

This study aims to generate induced human Schwann cells through direct reprogramming of fibroblasts using a non-integrating lentiviral (NILV) vector system. By comparing integrated and non-integrated lentiviral vectors for delivering EGR2 and SOX10, this research seeks to establish a safer, scalable approach for generating Schwann cells—bridging the gap between limited primary cell cultures and the demand for Schwann cells in peripheral nerve regeneration therapies.

MATERIALS AND METHODS

Lentiviral Plasmid Construction

The lentiviral vector backbone pLV-EF1a-IRES-PURO (Addgene #85132) was linearized using BamHI and EcoRI restriction sites. Synthesized plasmids carrying full length SOX10 (NM_006941.4), EGR2 (NM_000399.5), and EGFP gene sequences were similarly digested using the same restriction enzymes, followed by purification via 1% agarose gel electrophoresis. The desired DNA fragments were then extracted using the MONARCH DNA Gel Extraction Kit. A ligation reaction was prepared using a 1:3 insert-to-vector ratio with T4 DNA ligase before being subjected to a standard transformation protocol into competent NEBStable E. coli cells via the heat shock method. Transformed bacteria were plated on LB agar containing 100 µg/mL ampicillin and incubated overnight at 37°C. Emerging bacterial colonies were picked and subjected to colony PCR using restriction enzyme site-specific and gene-specific primers at both the 5′ and 3′ ends. For colony PCR, the following sequences were used: SOX10_BamHI_F (5′-TGGAATTTGCCCTTTTTGAG-3′), SOX10_BamHI_R (5′-CTGCTCCTTCTTGACCTTGC-3′), SOX10_EcoRI_F (5′-TCTACACGGCCATCTCTGAC-3′_, SOX10_EcoRI_R (5′-ACACCGGCCTTATTCCAAG-3′_, EGR2_BamHI_F (5′-TGGAATTTGCCCTTTTTGAG-3′), EGR2_BamHI_R (5′-TTGGGAAAGATGGTCACCGA-3′), EGR2_EcoRI_F (5′-CAGCAGTAACAGCAGCAGTC-3′_, EGR2_EcoRI_R (5′-ACACCGGCCTTATTCCAAG-3′). Positive clones were further verified by restriction enzyme digestion using BamHI and EcoRI, followed by agarose gel electrophoresis to confirm expected band sizes. Plasmid DNA from verified clones was extracted using the MONARCH Plasmid Miniprep Kit and further validated via Sanger sequencing to ensure the correct gene insert.

Cell Culture

Lenti-X 293T cells (Takara Bio) were cultured in complete DMEM medium containing 4 mM GlutaMAX, 4.5 g/L D-glucose, 0.1 mM MEM non-essential amino acids, 1 mM sodium pyruvate (Gibco), and 10% fetal bovine serum (FBS, Gibco). BJ human neonatal foreskin fibroblasts (ATCC) were maintained in the same complete DMEM medium supplemented with 10% FBS. All cell lines were incubated at 37°C in a humidified atmosphere containing 5% CO_2.

Lentiviral Production and Titration

Lentiviral vectors carrying SOX10, EGR2, and EGFP were packaged into lentiviral particles using either the VSV-G or Integrase-Deficient Lenti-X Packaging Single Shot system (Takara Bio USA). Lentiviral stocks were prepared following the protocol by Idris et al. (19) and concentrated 100-fold in serum-free DMEM before being aliquoted and stored at -80°C. To determine viral titers and validate the non-integrating properties of NILVs, Lenti-X 293T cells were transduced with serial dilutions of LV-EGFP for 72 hours. Flow cytometry analysis was performed to quantify the percentage of GFP-positive cells, with non-transduced cells serving as a negative control.

Lentiviral Transduction of BJ Fibroblasts

BJ fibroblasts were seeded in complete DMEM medium supplemented with 10% FBS and allowed to adhere overnight. Cells were transduced with LV or NILV carrying SOX10 and EGR2 at a multiplicity of infection (MOI) of 5 in the presence of polybrene. After 72 hours, the viral supernatant was removed and replaced with Schwann cell differentiation medium, consisting of DMEM, 10% FBS, L-glutamine, 2.5 µM forskolin, 2.5 ng/mL heregulin-β1 (HRG-β1), and 10 ng/mL basic fibroblast growth factor (bFGF). The culture medium was refreshed every 2–3 days, and cells were maintained for 21 days. Morphological changes were monitored daily under an EVOS M5000 fluorescent microscope.

Immunofluorescence Staining

For immunofluorescence analysis, transduced cells were fixed at the designated time points with 4% paraformaldehyde (PFA) for 20 minutes, followed by permeabilization with 0.1% Triton X-100 for 10 minutes. Cells were blocked with 10% normal horse serum (Vector Laboratories) for 1 hour before incubation with primary antibodies against SOX10 (rabbit monoclonal, Abcam, Cat #ab227684) at a 1:200 dilution, EGR2 (rabbit polyclonal, Invitrogen, Cat #PA5-112409) at a 1:200 dilution, and S100 (rabbit ploYclonal, DAKO, Cat #Z0311) at a 1:200 dilution overnight at 4°C. After washing, cells were incubated for 1 hour at room temperature with horse anti-mouse IgG (H+L) DyLight® 549 (1:500, Vector Laboratories,

Cat # VEL.DI-2549-1.5) and horse anti-rabbit IgG (H+L) DyLight® 488 (1:500, Vector Laboratories, Cat # VEL. DI-1088-1.5) as secondary antibodies. DAPI-containing Vectashield mounting medium (Vector Laboratories, Cat # VEL.H-1700-10) was used to counterstain nuclei. Fluorescent images were captured using an EVOS M5000 microscope, and image analysis was performed using ImageJ software.

Western Blotting

For western blot analysis, transduced cells were lysed in RIPA buffer, and protein concentration was determined using the Bradford assay. A total of 10 µg of protein was resolved via SDS-PAGE and transferred onto a PVDF membrane. The membrane was blocked with 5% non-fat dry milk and incubated with primary antibodies against SOX10 and EGR2 overnight at 4°C. After washing, membranes were incubated with horseradish peroxidase (HRP)-conjugated goat anti-mouse IgG (H+L) or goat anti-rabbit IgG (H+L) secondary antibodies. Protein bands were detected using an enhanced chemiluminescence (ECL) reagent and visualized with an Amersham 5000 imaging system.

RESULTS

Cloning of Lentiviral Vectors Carrying SOX10 and EGR2

Lentiviral vectors were cloned using restriction enzyme (RE) cloning with BamHI and EcoRI at the 5′ and 3′ ends of the pLV-EF1a-IRES-Puro backbone (Figure 1A). SOX10 and EGR2 gene inserts were synthesized with

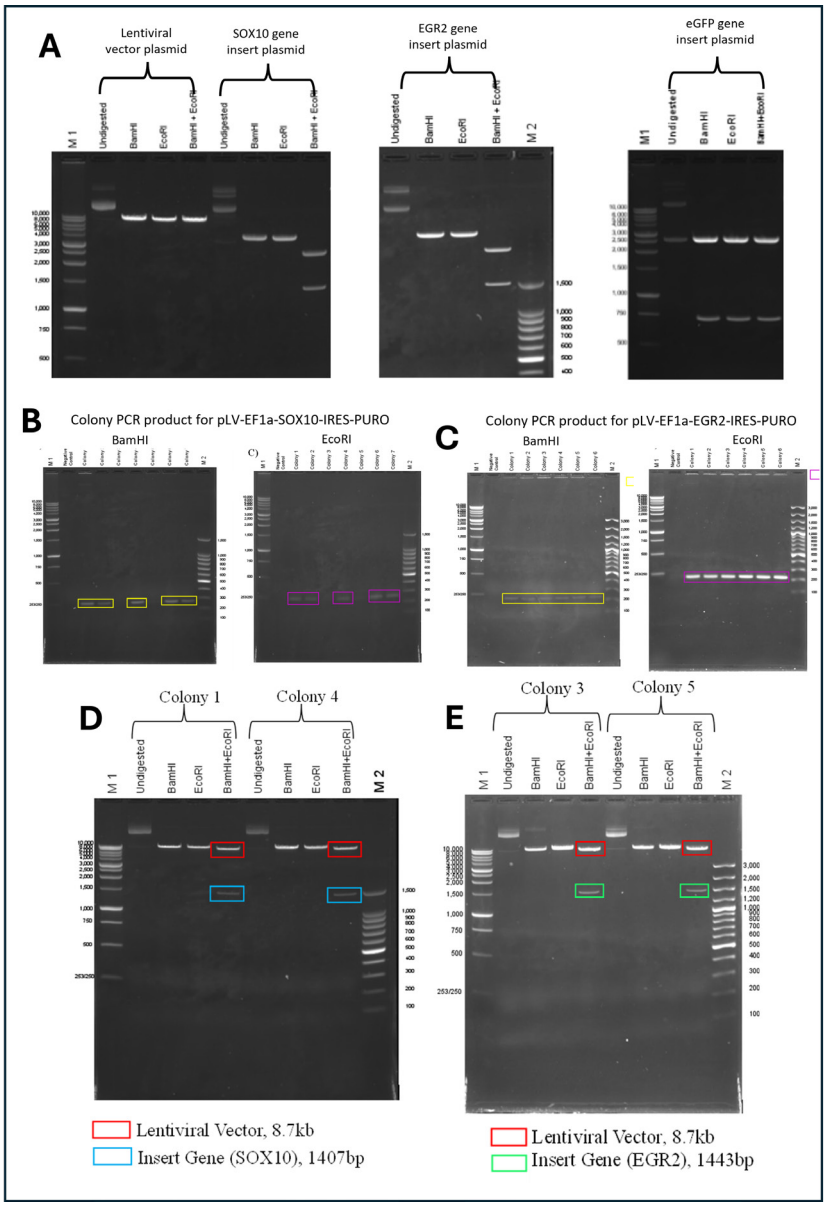

Fig. 1: Agarose gel electrophoresis (1% agarose) of lentiviral transfer vector plasmid (pLV-EF1a-IRES-PURO), SOX10 gene insert plasmid (pUC57_SOX10), EGR2 gene insert plasmid (pUC57_EGR2) and eGFP gene insert plasmid (pUC57_eGFP) were digested with restriction enzymes. M1 = 1kb DNA ladder, M2 = 100bp DNA ladder (A). Colony PCR product for pLV-EF1a-SOX10-IRES-PURO after ligation and transformation at the BamHI and EcoRI restriction sites on 1% agarose gel (B). Colony PCR product for pLV-EF1a-EGR2-IRES-PURO after ligation and transformation at at the BamHI and EcoRI restriction sites on 1% agarose gel (C). RE digestion of lentiviral plasmid; pLV-EF1a-SOX10-IRES-PURO at the BamHI and EcoRI restriction sites on 1% agarose gel (D). RE digestion of lentiviral plasmid; pLV-EF1a-EGR2-IRES-PURO at the BamHI and EcoRI restriction sites on 1% agarose gel (E).

matching RE sites. Following ligation, the constructs were transformed into E. coli (NEBStable). Seven colonies were selected for colony PCR validation to confirm correct orientation and insertion (Figure 1B-C). Colonies with expected PCR band sizes underwent RE digestion for further verification (Figure 1D-E). Sanger sequencing confirmed the integrity of the cloned inserts (Appendix).

Transient Expression of SOX10, EGR2, and EGFP in HEK293T Cells

To assess the functionality of the constructed vectors, HEK293T cells were transfected with pLV-EF1a-SOX10-IRES-PURO, pLV-EF1a-EGR2-IRES-PURO, and pLV-EF1a-eGFP-IRES-PURO (control). Western blot analysis confirmed SOX10 (49 kDa) and EGR2 (53 kDa) expression at 72 hours post-transfection (Figure 2A-B). GFP fluorescence was also observed, confirming successful transgene expression in LentiX-293T cells (Figure 2C).

Production and Validation of NILVs Carrying SOX10 and EGR2

To generate non-integrating lentiviruses (NILVs), SOX10 and EGR2 vectors were packaged using an integrase-deficient fourth-generation lentiviral system. NILV-EGFP was produced in parallel for viral titer estimation. Flow cytometry analysis of NILV-EGFP-transduced LentiX-293T cells determined a mean viral titer of 3.1×10^6 TU/mL across three independent experiments.

To validate NILV non-integration, BJ fibroblasts were transduced with either LV-GFP or NILV-EGFP and monitored for fluorescence over 14 days (Figure 3A). LV-GFP transduced cells showed consistent GFP expression, whereas a gradual decline in GFP expression was observed in NILV-GFP transduced cells, with complete loss by day 12, confirming episomal rather than chromosomal transgene expression (Figure 3B).

Transgene Expression of SOX10 and EGR2 in BJ Fibroblasts

Immunofluorescence staining at 72 hours post-transduction showed successful SOX10 (Figure 4) and EGR2 (Figure 5) expression in BJ fibroblasts. However, SOX10 expression was relatively low in both LV-SOX10 and NILV-SOX10 transduced cells, suggesting suboptimal transduction efficiency. In contrast, EGR2 expression was prominent in both LV-EGR2 and NILV-EGR2 groups, with nuclear localization confirmed via DAPI staining.

Reprogramming of BJ Fibroblasts into Schwann Cells

BJ fibroblasts were transduced with NILV-SOX10 and NILV-EGR2 for 21 days to assess Schwann cell reprogramming. Immunocytochemistry for S100β, a Schwann cell marker, was performed at 14 and 21 days post-transduction (PTD-14 and PTD-21) (Figure 6). At PTD-14, robust S100β expression suggested successful induction of Schwann cell-like phenotypes. However, by PTD-21, a marked decline in S100β expression was observed, indicating a potential inability to sustain Schwann cell-like characteristics over extended culture duration.

DISCUSSION

This study aims to establish a robust method for generating human Schwann cells for peripheral nerve research using non-integrating lentiviral vectors (NILVs),

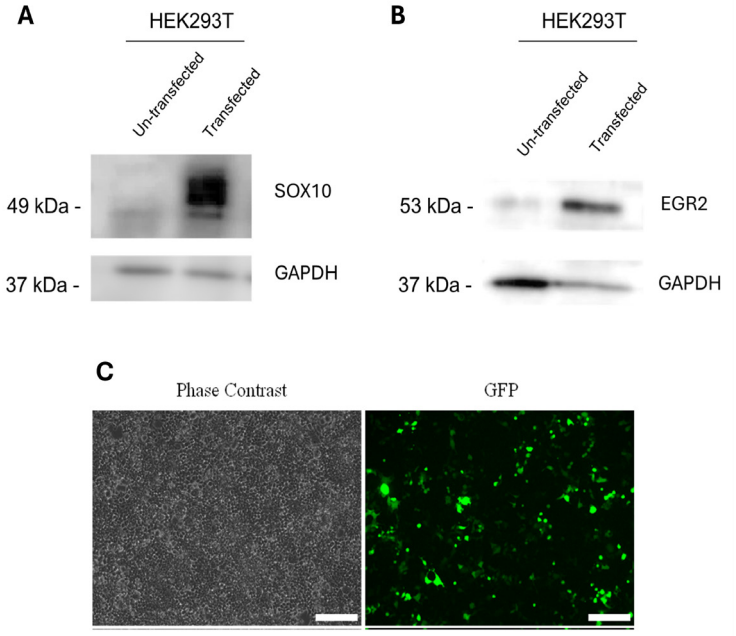

Fig. 2: Transient Expression of SOX10, EGR2, and EGFP in HEK293T Cells. Western blot analysis of transfected Lenti-X293T cells with a lentiviral plasmid carrying SOX10 (A) and EGR2 (B) genes at 72 hours post-transfection. Fluorescence image of transfected Lenti-X293T cells with a lentiviral plasmid eGFP at 72 hours post-transfection. Scale bar: 200µm (C).

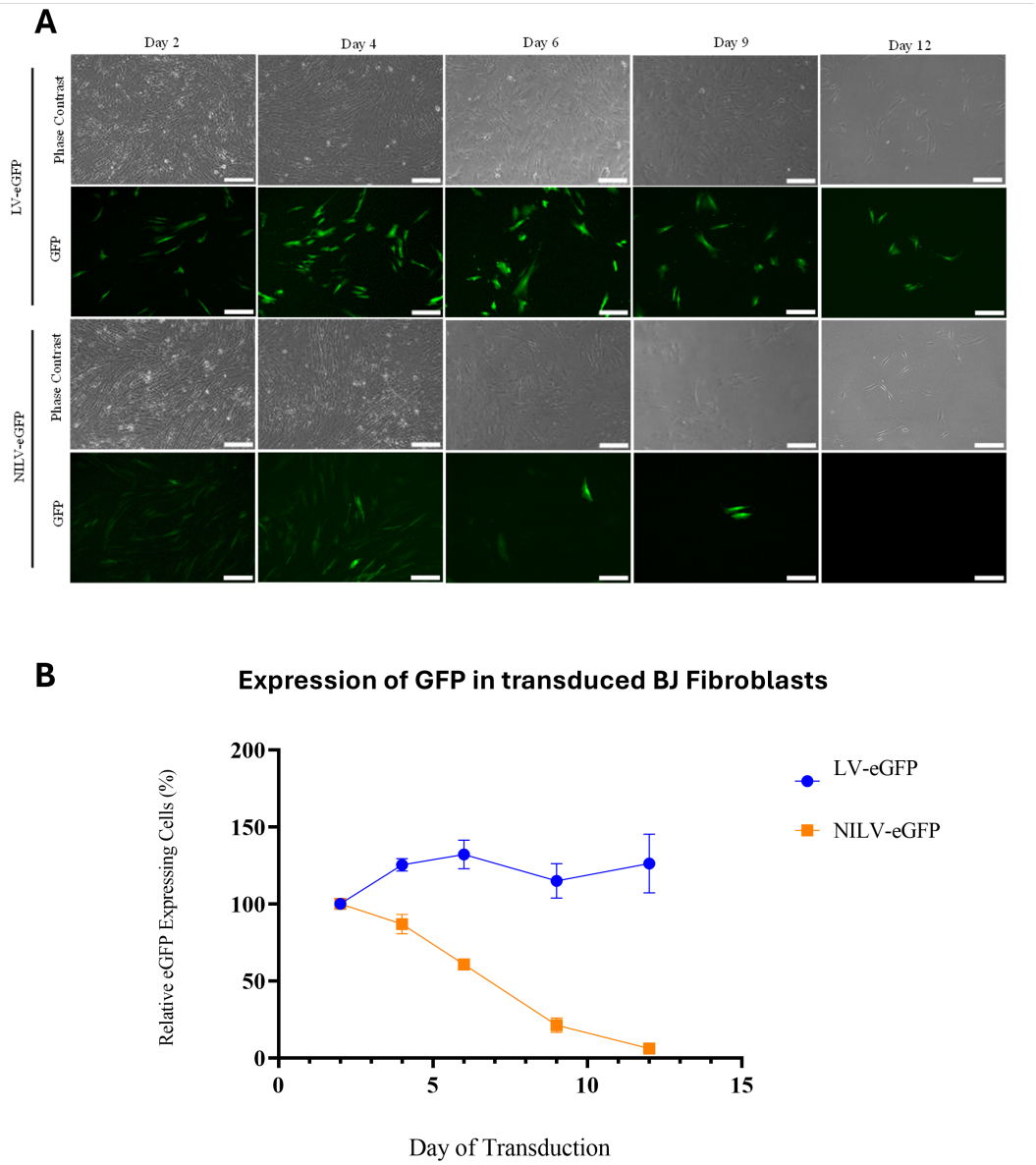

Fig. 3: Representative images of eGFP expression over time in BJ cells transduced with LV-eGFP (row 1 and 2) and NILV-eGFP (row 3 and 4). Scale Bar:200μM (A). Relative percentage of eGFP expression in BJ cells transduced with LV-eGFP and NILV-eGFP over time. The expression level of eGFP was observed by flow cytometry analysis on days 2, 4, 6, 9, and 12. The value represents the means (%) ± SD of triplicate wells (B).

which can transduce both dividing and non-dividing cells (19). We first developed a lentiviral plasmid encoding SOX10 and EGR2, two transcription factors essential for neural crest development, Schwann cell differentiation, and myelination (20). Lentiviruses carrying these genes were produced, and their transduction efficiency was assessed before proceeding with cell reprogramming. The efficacy of NILVs in direct reprogramming of human fibroblasts into Schwann cells was evaluated based on transgene expression and continuous culture over three weeks.

To compare the stability of transgene expression, we used eGFP as a surrogate marker in both integrating lentiviral vectors (LVs) and NILVs. Our results revealed a significant difference in long-term expression stability. In NILV-transduced BJ fibroblasts, eGFP expression and fluorescence intensity gradually declined after two weeks in culture compared to LV transduced cells that showed sustained eGFP expression over three weeks. Unlike traditional LVs that integrate into the host genome of the transduced cells, NILVs do not. Instead they rely on episomal DNA for transgene expression, reducing the risk of insertional mutagenesis (21). While integrating LVs will be passed onto the daughter cells during cell devision, the stability of episomal DNA expression in NILV transduced cells is limited, as it can be diluted through cell division, particularly in rapidly proliferating cells like BJ fibroblasts (22).

Despite these challenges, NILVs successfully delivered SOX10 and EGR2 genes, with EGR2 showing stronger expression than SOX10. These transcription factors play key roles in Schwann cell development, where SOX10

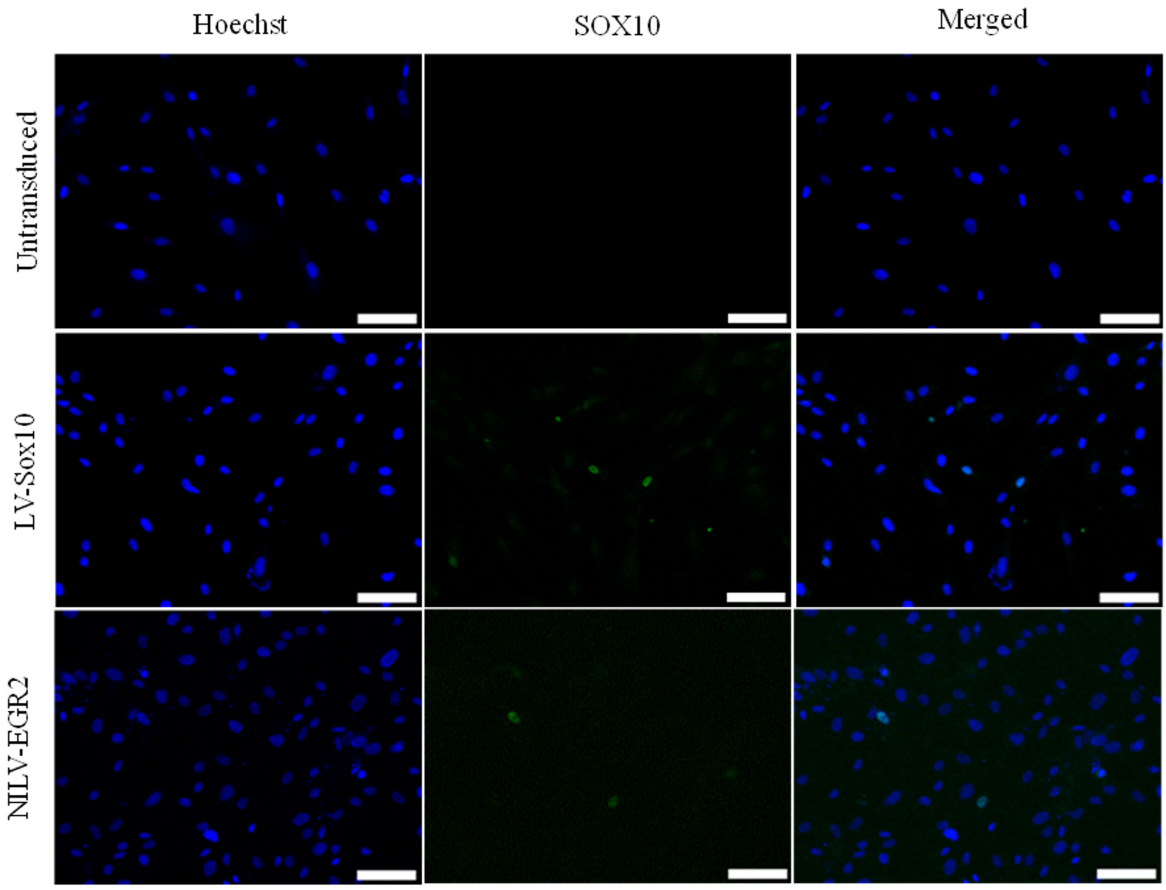

Fig. 4: Representative Immunofluorescence Imaging of SOX10 in LV and NILV transduced BJ cells. Fluorescence images were acquired at 72 hours post-transduction. BJ cells were stained with Hoechst and Sox10 antibodies. Scale bar:100µM.

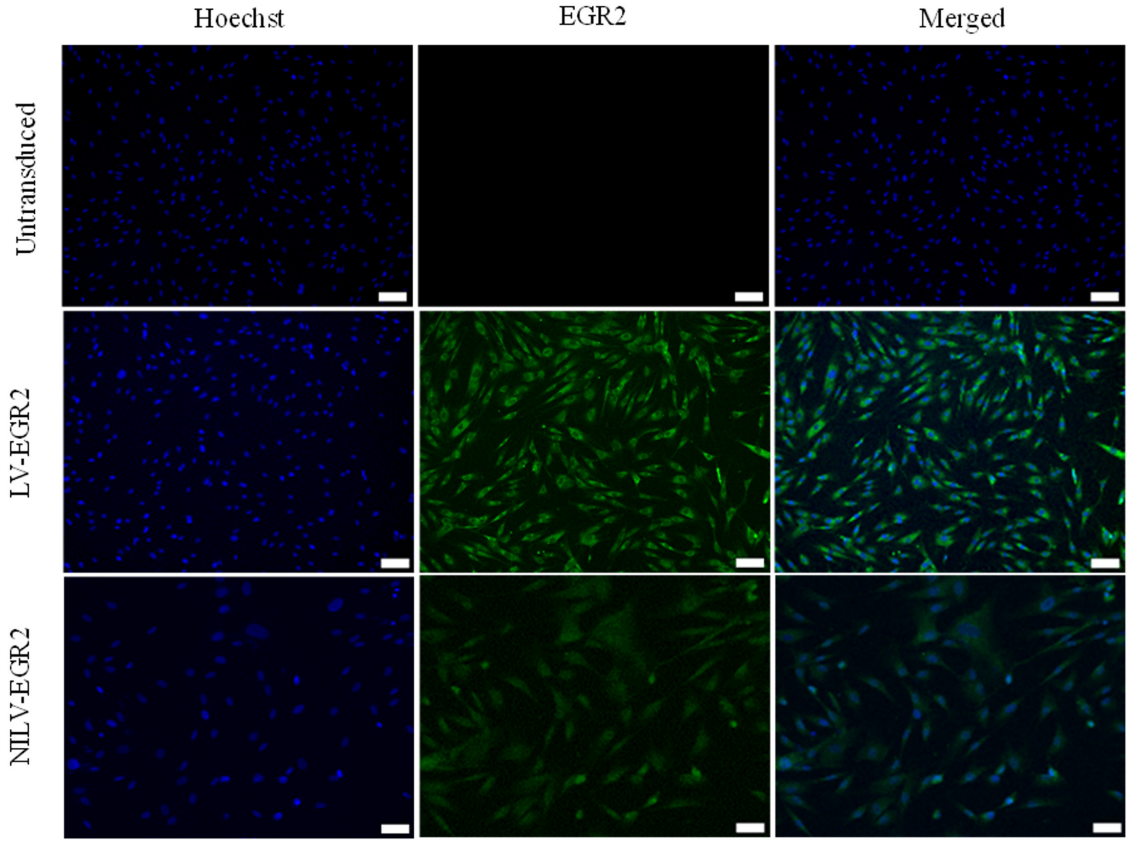

Fig. 5: Representative Immunofluorescence Imaging of EGR2 in LV and NILV transduced BJ cells. Fluorescence images were acquired at 72 hours post-transduction. BJ cells were stained with Hoechst and EGR2 antibodies Scale bar:50µM.

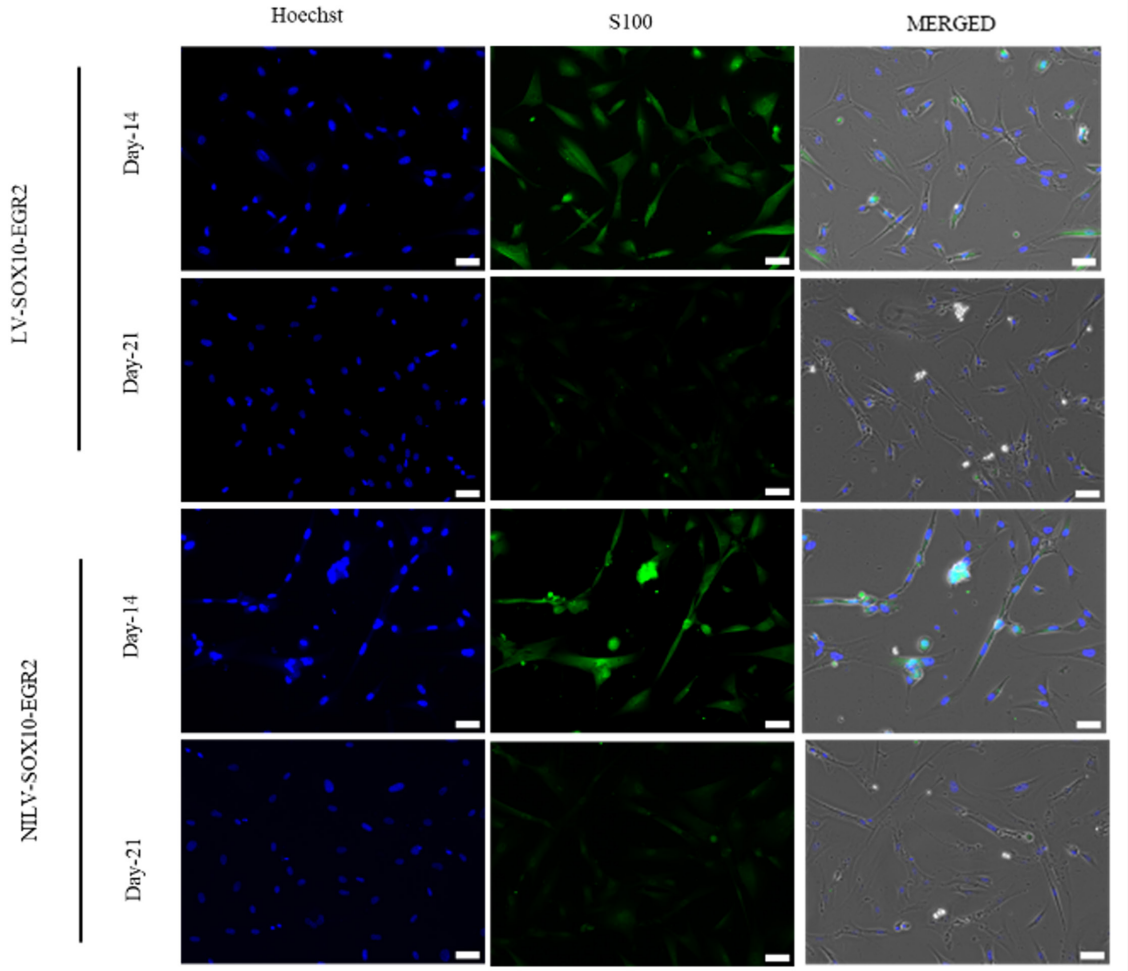

Fig. 6: Immunofluorescence micrographs of Induced Schwann cell cultured in Schwann cells medium for 21 days. The Induced Schwann cells were stained with Hoechst and EGR2 at PTD-14 and PTD-21. Scale bar = 50 µM

initiates and maintains the Schwann cell lineage, while EGR2 is crucial for myelination (14). NILV-mediated transduction induced Schwann cell-like characteristics in fibroblasts, as indicated by elevated expression of the Schwann cell marker S100β, similar to findings seen in LV-mediated transduction. This aligns with findings from Sowa et al. (2017), who achieved a 43% fibroblast-to-Schwann cell conversion rate using similar transcription factors (17).

Despite the successful expression of Schwann cell-specific markers in cells transduced using NILVs—indicating NILVs as a potential reprogramming strategy comparable to LVs—the Schwann cell-like phenotype could not be maintained over extended culture periods. This loss of phenotype may reflect insufficient transgene expression or instability of Schwann cell commitment in the absence of sustained signalling. One potential strategy to improve phenotypic stability involves increasing the viral load during transduction to enhance the overall copy number and expression of the delivered gene(s). Alternatively, employing stronger constitutive promoters such as cytomegalovirus (CMV) or phosphoglycerate kinase (PGK) could improve transcriptional activity and reinforce Schwann cell identity by driving more robust and sustained transgene expression (23). These modifications may help to overcome the limitations associated with transient expression in NILV systems and facilitate more stable lineage specification. While our study confirms the feasibility of NILV-mediated Schwann cell reprogramming, maintaining Schwann cell-like phenotypes remains a challenge for both integrating and non-integrating lentiviral approaches, warranting further investigation.

CONCLUSION

This study successfully demonstrated the feasibility of generating human Schwann cells through direct reprogramming of fibroblasts using non-integrating lentiviral vectors (NILVs) carrying SOX10 and EGR2. Lentiviral vectors were efficiently cloned, validated, and expressed in HEK293T cells, confirming their functionality. NILV-mediated transduction in BJ fibroblasts resulted in detectable expression of SOX10 and EGR2, with EGR2 exhibiting stronger expression. Immunocytochemistry analysis revealed that NILV-induced Schwann cell-like phenotypes, as indicated by S100β expression, were evident at 14 days post-transduction but declined by day 21, suggesting challenges in maintaining Schwann cell identity over prolonged culture.

While NILVs provide a safer alternative to integrating vectors by minimizing genomic insertion risks, their episomal nature resulted in gradual transgene loss over time. This highlights the need for further optimization to enhance transgene stability and improve Schwann cell lineage maintenance. Future studies should explore alternative delivery strategies or supportive culture conditions to sustain Schwann cell-like properties for extended periods. Overall, this study provides valuable insights into NILV-based Schwann cell reprogramming, bridging the gap between primary Schwann cell limitations and the need for scalable cell sources in peripheral nerve research and regenerative therapies.

ACKNOWLEDGMENTS

We would like to thank the Director General of Health Malaysia for his approval to publish this article, the Director of Institute for Medical Research and staff of Institute for Medical Research and Institute of Medical Science Technology, Universiti Kuala Lumpur for their support throughout the course of this research. This research was funded by the Fundamental Research Grant Scheme (FRGS/1/2024/SKK10/UNIKL/02/2) from the Ministry of Higher Education (MOHE) and the Ministry of Health (MOH), Malaysia (NMRR ID-22-00052-UOW).

REFERENCES

1. Feltri ML, Poitelon Y, Previtali SC. How Schwann Cells Sort Axons: New concepts. Neuroscientist. 2016;22:252–65.
2. Sardella-Silva G, Mietto BS, Ribeiro-Resende VT. Four Seasons for Schwann Cell Biology, Revisiting Key Periods: Development, Homeostasis, Repair, and Aging. Biomolecules 2021, Vol 11, Page 1887 [Internet]. 2021 [cited 2025 Feb 24];11:1887. Available from: https://www.mdpi.com/2218-273X/11/12/1887/htm
3. Rinwa P, Calvo-Enrique L, Zhang MD, Nyengaard JR, Karlsson P, Ernfors P. Demise of nociceptive Schwann cells causes nerve retraction and pain hyperalgesia. Pain [Internet]. 2021 [cited 2025 Feb 24];162:1816–27. Available from: https://journals.lww.com/pain/fulltext/2021/06000/demise_of_nociceptive_schwann_cells_causes_nerve.24.aspx
4. Darabid H, St-Pierre-See A, Robitaille R. Purinergic-Dependent Glial Regulation of Synaptic Plasticity of Competing Terminals and Synapse Elimination at the Neuromuscular Junction. Cell Rep [Internet]. 2018 [cited 2025 Feb 24];25:2070-2082.e6. Available from: http://www.cell.com/article/S2211124718316796/fulltext
5. Zhang SH, Shurin G V., Khosravi H, Kazi R, Kruglov O, Shurin MR, et al. Immunomodulation by Schwann cells in disease. Cancer Immunology, Immunotherapy 2019 69:2 [Internet]. 2019 [cited 2025 Feb 24];69:245–53. Available from: https://link.springer.com/article/10.1007/s00262-019-02424-7
6. Boerboom A, Dion V, Chariot A, Franzen R. Molecular mechanisms involved in schwann cell plasticity. Front Mol Neurosci [Internet]. 2017 [cited 2020 Sep 25];17:38. Available from: https://pubmed.ncbi.nlm.nih.gov/28261057/
7. Balakrishnan A, Belfiore L, Chu TH, Fleming T, Midha R, Biernaskie J, et al. Insights Into the Role and Potential of Schwann Cells for Peripheral Nerve Repair From Studies of Development and Injury. Front Mol Neurosci [Internet]. 2021 [cited 2025 Feb 24];13:608442. Available from: www.frontiersin.org
8. Abd Razak NH, Idris J, Hassan NH, Zaini F, Muhamad N, Daud MF. Unveiling the Role of Schwann Cell Plasticity in the Pathogenesis of Diabetic Peripheral Neuropathy. International Journal of Molecular Sciences 2024, Vol 25, Page 10785 [Internet]. 2024 [cited 2025 Feb 24];25:10785. Available from: https://www.mdpi.com/1422-0067/25/19/10785/htm
9. Gersey ZC, Burks SS, Anderson KD, Dididze M, Khan A, Dietrich WD, et al. First human experience with autologous Schwann cells to supplement sciatic nerve repair: report of 2 cases with long-term follow-up. Neurosurg Focus [Internet]. 2017 [cited 2025 Feb 24];42. Available from: https://pubmed.ncbi.nlm.nih.gov/28245668/
10. Negro S, Pirazzini M, Rigoni M. Models and methods to study Schwann cells. J Anat [Internet]. 2022 [cited 2025 Feb 24];241:1235–58. Available from: https://onlinelibrary.wiley.com/doi/full/10.1111/joa.13606
11. Zhou LN, Cui XJ, Su KX, Wang XH, Guo JH. Beneficial reciprocal effects of bone marrow stromal cells and Schwann cells from adult rats in a dynamic co culture system in vitro without intercellular contact. Mol Med Rep [Internet]. 2015 [cited 2025 Feb 25];12:4931–8. Available from: https://pubmed.ncbi.nlm.nih.gov/26133460/
12. Tetzlaff W, Okon EB, Karimi-Abdolrezaee S, Hill CE, Sparling JS, Plemel JR, et al. A systematic review of cellular transplantation therapies for spinal cord injury. J Neurotrauma [Internet]. 2011 [cited 2025 Feb 25];28:1611–82. Available from: https://pubmed.ncbi.nlm.nih.gov/20146557/
13. Zakrzewski W, Dobrzyński M, Szymonowicz M, Rybak Z. Stem cells: Past, present, and future. Stem Cell Res Ther [Internet]. 2019 [cited 2025 Feb 25];10:1–22. Available from: https://stemcellres.biomedcentral.com/articles/10.1186/s13287-019-1165-5
14. Monje M. Myelin Plasticity and Nervous System Function. Annu Rev Neurosci [Internet]. 2018 [cited 2025 Feb 25];41:61–76. Available from: https://pubmed.ncbi.nlm.nih.gov/29986163/
15. Rai N, Singh AK, Singh SK, Gaurishankar B, Kamble SC, Mishra P, et al. Recent technological advancements in stem cell research for targeted

therapeutics. Drug Deliv Transl Res [Internet]. 2020 [cited 2025 Feb 25];10:1147–69. Available from: https://pubmed.ncbi.nlm.nih.gov/32410157/
16. Ruiz S, Lopez-Contreras AJ, Gabut M, Marion RM, Gutierrez-Martinez P, Bua S, et al. Limiting replication stress during somatic cell reprogramming reduces genomic instability in induced pluripotent stem cells. Nat Commun [Internet]. 2015 [cited 2025 Feb 25];6. Available from: https://pubmed.ncbi.nlm.nih.gov/26292731/
17. Sowa Y, Kishida T, Tomita K, Yamamoto K, Numajiri T, Mazda O. Direct Conversion of Human Fibroblasts into Schwann Cells that Facilitate Regeneration of Injured Peripheral Nerve In Vivo. Stem Cells Transl Med [Internet]. 2017 [cited 2025 Feb 25];6:1207–16. Available from: https://pubmed.ncbi.nlm.nih.gov/28186702/
18. Kim HS, Kim JY, Song CL, Jeong JE, Cho YS. Directly induced human Schwann cell precursors as a valuable source of Schwann cells. Stem Cell Res Ther [Internet]. 2020 [cited 2025 Feb 25];11:257. Available from: https://stemcellres.biomedcentral.com/articles/10.1186/s13287-020-01772-x
19. Mohd Idris I, Nordin F, Muhamad NJ, Jalil JA, Amin Nordin FD, Mohamed R, et al. The Establishment of In Vitro Human Induced Pluripotent Stem Cell-Derived Neurons. Sains Malays. 2023;52:863–76.
20. Wang X, Ma C, Rodrнguez Labrada R, Qin Z, Xu T, He Z, et al. Recent advances in lentiviral vectors for gene therapy. Science China Life Sciences 2021 64:11 [Internet]. 2021 [cited 2025 Feb 27];64:1842–57. Available from: https://link.springer.com/article/10.1007/s11427-021-1952-5
21. Tammia M, Mi R, Sluch VM, Zhu A, Chung T, Shinn D, et al. Egr2 overexpression in Schwann cells increases myelination frequency in vitro. Heliyon [Internet]. 2018 [cited 2025 Feb 27];4:e00982. Available from: https://www.cell.com/action/showFullText?pii=S240584401832677X
22. Mulia GE, Picanзo-Castro V, Stavrou EF, Athanassiadou A, Figueiredo ML. Advances in the Development and the Applications of Nonviral, Episomal Vectors for Gene Therapy. Hum Gene Ther [Internet]. 2021 [cited 2025 Feb 27];32:1076–95. Available from: https://www.liebertpub.com/doi/10.1089/hum.2020.310
23. Chavez M, Rane DA, Chen X, Qi LS. Stable expression of large transgenes via the knock-in of an integrase-deficient lentivirus. Nature Biomedical Engineering 2023 7:5 [Internet]. 2023 [cited 2025 Feb 27];7:661–71. Available from: https://www.nature.com/articles/s41551-023-01037-x
24. Naldini L. Gene therapy returns to centre stage. Nature [Internet]. 2015 [cited 2025 May 30];526:351–60. Available from: https://www.nature.com/articles/nature15818